



TECHNISCHE UNIVERSITÄT CHEMNITZ

## **Sonderforschungsbereich 393**

Parallele Numerische Simulation für Physik und Kontinuumsmechanik

Helmut Harbrecht

Ulf Kähler

Reinhold Schneider

### **Wavelet Galerkin BEM on unstructured meshes**

Preprint SFB393/04-06

Preprintreihe des Chemnitzer SFB 393

ISSN 1619-7178 (Print)

ISSN 1619-7186 (Internet)

**SFB393/04-06**

**Mai 2004**

## CONTENTS

Introduction	1
1. Problem formulation and preliminaries	2
1.1. Boundary integral equations	2
1.2. Discretization	3
2. Wavelet bases	5
2.1. Cluster tree	5
2.2. Construction of wavelets	6
2.3. Discrete wavelet transform	12
3. The wavelet Galerkin scheme	12
3.1. Wavelet matrix compression	12
3.2. Setting up the matrix pattern	15
3.3. Computing the compressed system matrix	15
4. Numerical results	17
References	20

Author's addresses:

H. Harbrecht, R. Schneider  
Christian–Albrechts–Universität zu Kiel  
Institut für Informatik und Praktische Mathematik  
Olshausenstr. 40  
D-24098 Kiel  
*hh@numerik.uni-kiel.de, rs@numerik.uni-kiel.de*

U. Kähler  
Technische Universität Chemnitz  
Fakultät für Mathematik  
Reichenhainerstr. 41  
D-09107 Chemnitz  
*ulka@mathematik.tu-chemnitz.de*

<http://www.tu-chemnitz.de/sfb393/>

## INTRODUCTION

Many mathematical models concerning e.g. field calculations, flow simulation, elasticity or visualization are based on operator equations with *global operators*, especially *boundary integral operators*. In general, traditional discretizations will lead to possibly very large linear systems with *densely populated* matrices. Therefore, the complexity for solving such equations is at least  $\mathcal{O}(N^2)$ , where  $N$  denotes the number of equations. This fact restricts the maximum size of the linear equations seriously.

Modern methods for the fast solution of boundary integral equations reduce the complexity to a suboptimal rate, i.e.  $\mathcal{O}(N \log^\alpha N)$ , or even an optimal rate, i.e.  $\mathcal{O}(N)$ . Prominent examples for such methods are the *fast multipole method* [10], the *panel clustering* [12], and related methods like  *$\mathcal{H}$ -matrices* [11], in particular the *adaptive cross approximation* [1]. *Wavelet matrix compression* [2] offers a further tool for the fast solution of integral equations. In fact, a Galerkin discretization with wavelet bases results in quasi-sparse matrices, i.e., most of the matrix coefficients are negligible and can be treated as zero. Discarding these nonrelevant matrix coefficients is called matrix compression. It has been shown in [7, 15] that only  $\mathcal{O}(N)$  significant matrix coefficients remain.

The major difficulty of the wavelet matrix compression is the construction of suitable wavelet bases. The common approach is based on refinement strategies which requires a parametric representation of the surface by smooth patches [6, 7, 15]. A novel wavelet construction, introduced and applied to the so-called nonstandard form of the system matrix in [17], employs a coarsening strategy of a given fine mesh which might be considered also unstructured. In the present paper we prove that these wavelet bases satisfy the approximation property and establish the inverse estimate with respect to the Sobolev spaces  $H^s(\Gamma)$  in the range  $|s| < 1/2$ . Hence, we derive the norm equivalence for all  $|s| < 1/2$ . This makes us possible to apply our concept of the wavelet matrix compression to the standard form of the system matrix. We prove that only  $\mathcal{O}(N \log N)$  matrix coefficients remain relevant, without deteriorating the stability and accuracy of the underlying Galerkin scheme. Using, similarly to [14], techniques from the fast multipole method and the panel clustering, the computation of the compressed system matrix can be performed within suboptimal complexity. Hence, the present method reduces the complexity considerably while preserving the advantage of an explicit system matrix. Moreover, the diagonal of the system matrix defines a good preconditioner in the case of integral operators of nonzero order [9, 14].

The outline of the present paper is as follows. First, in Section 1, we introduce the class of problems under consideration. Then, in Section 2 we introduce the wavelet bases and prove the desired norm equivalences. The present analysis shows that the wavelet preconditioning for the single layer operator is nearly optimal. With such bases at hand we are able to introduce the fully discrete wavelet Galerkin scheme in Section 3. In Section 4 we present numerical results in order to demonstrate our algorithm.

## 1. PROBLEM FORMULATION AND PRELIMINARIES

**1.1. Boundary integral equations.** In the present paper we consider the fast solution of a boundary integral equation on the closed Lipschitz surface  $\Gamma$  of an  $(n+1)$ -dimensional domain  $\Omega \subset \mathbb{R}^{n+1}$

$$(1.1) \quad Au = f \quad \text{on } \Gamma.$$

The inner product in  $L^2(\Gamma)$  will be denoted by

$$(1.2) \quad \langle u, v \rangle := \int_{\Gamma} v(x)u(x)d\Gamma.$$

Moreover, for  $|s| < 3/2$  we define the Sobolev spaces  $H^s(\Gamma)$  locally by Lipschitz continuous coordinates. The associated norms are indicated by  $\|\cdot\|_s$ .

The boundary integral operator

$$(Au)(x) = \int_{\Gamma} k(x, y)u(y)d\Gamma_y$$

is assumed to be a strictly coercive operator of order  $2q$ , that is  $A : H^q(\Gamma) \rightarrow H^{-q}(\Gamma)$  with

$$\langle Au, u \rangle \gtrsim \|u\|_q^2.$$

This property is up to well known modifications valid for the single layer operator with  $q = -1/2$ . Though, for general Lipschitz domains, the double layer operator is not always coercive, in many cases it is. So we assume that the double layer operator satisfies this assertion with  $q = 0$ .

We shall further assume throughout this paper that the kernel function  $k(x, y)$  under consideration is an analytic function in the *space* variables  $x, y \in \mathbb{R}^{n+1}$ , apart from the singularity  $x = y$ . More precisely, we assume that the kernel function satisfies the following decay property

$$(1.3) \quad |\partial_x^\alpha \partial_y^\beta k(x, y)| \lesssim \frac{\alpha! \beta!}{(s \|x - y\|)^{n+2q+|\alpha|+|\beta|}}, \quad s > 0,$$

uniformly in the  $(n+1)$ -dimensional multi-indices  $\alpha = (\alpha_1, \dots, \alpha_{n+1})$  and  $\beta = (\beta_1, \dots, \beta_{n+1})$ .



Under the assumption (1.3), we can expand the kernel in a convergent Taylor series with center  $(x_0, y_0) \in \mathbb{R}^{n+1} \times \mathbb{R}^{n+1}$ . Consider  $r_x, r_y \in \mathbb{R}$  such that  $\|x_0 - y_0\| > r_x + r_y$ , then for all  $x, y \in \mathbb{R}^{n+1}$  satisfying  $\|x - x_0\| < r_x, \|y - y_0\| < r_y$  we have

$$(1.4) \quad k(x, y) = \sum_{|\alpha|, |\beta| < p} \frac{\partial_x^\alpha \partial_y^\beta k(x_0, y_0)}{\alpha! \beta!} (x - x_0)^\alpha (y - y_0)^\beta + R_{(x_0, y_0)}^{(p)}(r_x, r_y)$$

with the error estimate

$$(1.5) \quad |R_{(x_0, y_0)}^{(p)}(r_x, r_y)| \lesssim \frac{\max\{r_x, r_y\}^p}{(s[\|x_0 - y_0\| - r_x - r_y])^{n+2q+2p}}.$$

Moreover, an *infinite* expansion in terms of

$$(1.6) \quad k(x, y) = \sum_{\min\{|\alpha|, |\beta|\} < p} \frac{\partial_x^\alpha \partial_y^\beta k(x_0, y_0)}{\alpha! \beta!} (x - x_0)^\alpha (y - y_0)^\beta + Q_{(x_0, y_0)}^{(p)}(r_x, r_y)$$

yields the error estimate

$$(1.7) \quad |Q_{(x_0, y_0)}^{(p)}(r_x, r_y)| \lesssim \frac{r_x^p r_y^p}{(s[\|x_0 - y_0\| - r_x - r_y])^{n+2q+2p}}.$$

In contrast to estimate (1.4), (1.5) the second estimate will give a much sharper bound of the decay of matrix coefficients. Therefore, this estimate is the key for a successful wavelet matrix compression.

We emphasize that one may consider any convergent expansion of the kernel different from the Taylor series (1.4). For example, in three dimensions ( $n = 2$ ) the common approach employs spherical harmonics instead of polynomials since less coefficients are required to achieve a certain accuracy in (1.5). Moreover, in case of double layer potentials some further modifications are required since the normal to the boundary appears in the kernel. For sake of clearness of presentation we have chosen the Taylor expansion. With some minor modifications our ideas are also applicable in the aforementioned cases.

**1.2. Discretization.** We shall be concerned with a Galerkin discretization of (1.1) based on lowest order boundary elements, that are piecewise constant ansatz functions. To this end, we suppose that the boundary  $\Gamma$  under consideration is given by a set of panels

$$\Gamma = \bigcup_{i=1}^N \pi_i,$$

where each  $\pi_i$  is an  $n$ -dimensional plane or even curved simplex in  $\mathbb{R}^{n+1}$ . More precisely, for each  $i$  a smooth diffeomorphism  $\kappa_i$  exists mapping a reference simplex to the panel  $\pi_i$ . The intersection of different simplices  $\pi_i \cap \pi_j$  is either empty or a lower dimensional face. Moreover, we consider the triangulation to be quasi uniform: Let  $\rho_i$  denote the  $n$ -dimensional inscribed ball of the simplex  $\pi_i$ , then the step width

$h_N := \max_{i=1}^N \text{diam}(\pi_i)$  scales proportionally and reciprocal proportionally with  $\rho_i$  and  $N$ , respectively,

$$\min_{i=1}^N \rho_i \sim h_N \sim N^{-1/n}.$$

Let us remark that the class of surface representations under consideration includes the case of an unstructured mesh with respect to parametric surfaces as well as polygonal approximations to a given surface. Moreover, it allows in a wide range of applications also the treatment of complex geometries.

On the given triangulation we consider the space of piecewise constant ansatz functions

$$V_N := \text{span}\{\phi_i : i = 1, 2, \dots, N\},$$

where each ansatz function is supported on a single simplex

$$(1.8) \quad \phi_i(x) = \begin{cases} 1/\sqrt{|\pi_i|}, & x \in \pi_i, \\ 0, & \text{elsewhere.} \end{cases}$$

The Galerkin scheme of (1.1) reads: Seek  $u_N \in V_N$  such that

$$(1.9) \quad \langle Au_N, v_N \rangle = \langle f, v_N \rangle \quad \text{for all } v_N \in V_N.$$

Equivalently, making the ansatz  $u_N = \sum_{i=1}^N u_i \phi_i$  we have to solve the linear system of equations

$$(1.10) \quad \mathbf{A}_N^\phi \mathbf{u}_N^\phi = \mathbf{f}_N^\phi$$

with the system matrix  $\mathbf{A}_N^\phi = [\langle A\phi_j, \phi_i \rangle]_{i,j=1}^N$ , the solution vector  $\mathbf{u}_N^\phi = [u_i]_{i=1}^N$  and the load vector  $\mathbf{f}_N^\phi = [\langle f, \phi_j \rangle]_{j=1}^N$ .

Denoting the exact solution of (1.1) by  $u$ , the traditional error analysis of the Galerkin scheme yields the well known error estimate on  $u_N$

$$\|u - u_N\|_q \lesssim h_N^{t-q} \|u\|_t$$

for  $q \leq t \leq 1$ . If we define the Sobolev spaces  $H^s(\Gamma)$  in the range  $-5/2 < s \leq 3/2$  by duality with respect to the  $H^{-1/2}(\Gamma)$ -inner product induced by the single layer operator  $V$ , that is

$$\|u\|_s := \sup_{\|v\|_{-(1+s)}=1} \langle Vu, v \rangle,$$

then we can apply Aubin-Nitsche's trick to obtain twice the convergence rate associated with the energy norm:

**Lemma 1.1.** *Let  $u$  be the solution of (1.1) and  $u_N$  the solution of the Galerkin scheme (1.10). Then, the following estimate*

$$(1.11) \quad \|u - u_N\|_s \lesssim h_N^{t-s} \|u\|_t$$

where  $2q - 1 \leq s < 1/2$ ,  $s \leq t$ ,  $q \leq t \leq 1$  holds uniformly in  $N$ , provided that  $u$  is regular enough. The values  $s = 2q - 1$  and  $t = 1$  lead to the highest rate of convergence  $h_N^{2(1-q)}$ .

Unfortunately, the Galerkin system (1.10) is densely populated if we use the traditional *single-scale basis*  $\{\phi_i\}$ . Hence, we will consider a different basis in the spaces  $V_N$ , namely a *wavelet basis*, which leads to a quasi-sparse system matrix. As we will see we can sparsify the system matrix without deteriorating the order of convergence given by (1.11).

## 2. WAVELET BASES

**2.1. Cluster tree.** In contrast to previous wavelet constructions we cannot use a refinement strategy since the representation of the geometry automatically limits the finest level of any finite consideration to a single simplex. Hence, we will employ a coarsening procedure to define a multiscale hierarchy

$$(2.12) \quad V_0 \subset V_1 \subset \cdots \subset V_J = V_N.$$

It will be realized by a uniform hierarchical non-overlapping subdivision of the boundary  $\Gamma$ , called the *cluster tree*.

A cluster  $\nu$  is defined as the nonempty union  $\nu = \pi_1 \cup \cdots \cup \pi_i$  of a certain set of simplices  $\pi_i$ . It is called the *father cluster* of  $\nu'$ , which will be denoted by  $\nu' \prec \nu$ , if  $\nu' \subsetneq \nu$  and no further cluster  $\nu''$  exists with  $\nu' \subsetneq \nu'' \subsetneq \nu$ . The cluster  $\nu'$  is then called a *son cluster* of  $\nu$ . If we order these clusters hierarchically concerning the father-son relation “ $\prec$ ” we arrive at a tree structure, the so-called cluster tree  $T$ .

We have to specify some properties of the cluster tree  $T$  in more detail:

- $\Gamma$  is the root of  $T$ .
- The leaves are the simplices  $\pi_i$ .
- The cluster  $\nu$  belongs to the level  $j$  if there exist  $j$  clusters  $\{\nu_i\}_{i=0}^{j-1}$  such that

$$\nu \prec \nu_{j-1} \prec \cdots \prec \nu_0 = \Gamma.$$

The root  $\Gamma$  of the cluster tree is of the level 0 and  $J$  is the maximal level. We denote the  $l$ -th cluster of the level  $j$  by  $\nu_{j,l}$ . The union of all clusters of a level  $j$  form a non-overlapping subdivision of the boundary  $\Gamma$

$$\bigcup_l \nu_{j,l} = \Gamma \quad \text{and} \quad \nu_{j,l}^\circ \cap \nu_{j,l'}^\circ = \emptyset, \quad l \neq l'.$$

- The cluster tree is approximately a balanced  $2^n$ -tree, which means that the number of sons  $k(\nu_{j,l})$  of the clusters  $\nu_{j,l}$  satisfies

$$k(\nu_{j,l}) \sim 2^n \quad \text{for all } \nu_{j,l} \in T \setminus \{\pi_i\}.$$

- The diameter of the clusters  $\nu_{j,l}$  is local with respect to the level  $j$  in terms of

$$\text{diam } \nu_{j,l} \sim 2^{-j}.$$

Moreover, the number  $\#\nu_{j,l}$  of simplices  $\pi_i$  contained in a cluster  $\nu_{j,l}$  from the level  $j$  scales approximately like  $2^{n(J-j)}$

$$\#\nu_{j,l} \sim 2^{n(J-j)}.$$

The cluster tree  $T$  with the indicated terms should be given for our further considerations. A common algorithm for its construction is based on a hierarchical subdivision of the  $(n+1)$ -space. We begin by embedding the boundary  $\Gamma$  in a top-level cube  $\nu_0$ . The cube is subsequently subdivided into  $2^{n+1}$  equal cubes and this process is iterated until a cube encloses less than a predetermined number of simplices, cf. Figure 2.1. Alternatively, one may also consider a cluster tree obtained by agglomeration starting on the finest grid.

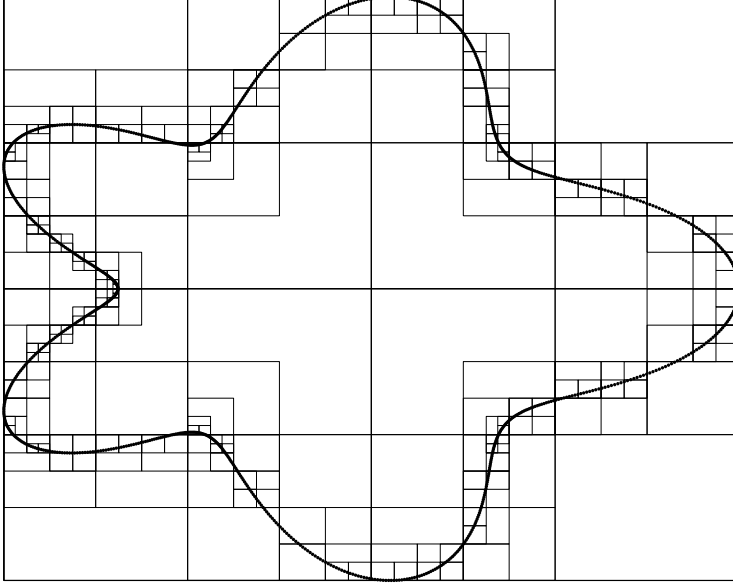


FIGURE 2.1. Clustering of a given surface.

**2.2. Construction of wavelets.** With the cluster tree at hand we are in the position to construct the wavelet basis. It should realize a hierarchical structure, which means that the support of wavelet from the level  $j$  should be restricted to a single

cluster from the level  $j$  to ensure the locality of the wavelets. Moreover, for matrix compression, the wavelets should provide *vanishing moments* of order  $\tilde{d}$ , that is

$$(2.13) \quad \int_{\Gamma} (x - x_0)^\alpha \psi_{j,k}(x) d\Gamma = 0, \quad |\alpha| < \tilde{d},$$

where  $x_0$  denotes the center of the associated cluster. We like to emphasize that  $(x - x_0)^\alpha$  is considered as a spatial polynomial in  $\mathbb{R}^{n+1}$  and only their traces on  $\Gamma$  enter in definition (2.13).

We consider a cluster  $\nu$  from the level  $j$  and define scaling functions  $\Phi_j^\nu = \{\phi_{j,k}^\nu\}$  and wavelets  $\Psi_j^\nu = \{\psi_{j,k}^\nu\}$  supported in this cluster as linear combinations from the scaling functions  $\Phi_{j+1}^\nu$  of  $\nu$ 's son clusters on the finer level  $j+1$

$$(2.14) \quad [\Phi_j^\nu, \Psi_j^\nu] = \Phi_{j+1}^\nu [V_{j,0}^\nu, V_{j,1}^\nu],$$

where the matrix  $[V_{j,0}^\nu, V_{j,1}^\nu]$  is supposed to be orthogonal. For the beginning of the recursion on the finest level  $J$  we have to use the piecewise constant ansatz functions supported on a single simplex  $\Phi_J^{\pi_i} = \{\phi_i\}$ . That way, we obtain the multiscale hierarchy (2.12) via

$$(2.15) \quad V_j := \text{span}\{\Phi_j^\nu : \nu \text{ is a cluster from the level } j\}.$$

Moreover, the spaces

$$W_j := \text{span}\{\Psi_j^\nu : \nu \text{ is a cluster from the level } j\}$$

satisfy

$$V_{j+1} = V_j \oplus^\perp W_j$$

due to the orthogonality of the matrix  $[V_{j,0}^\nu, V_{j,1}^\nu]$ .

In order to realize (2.13) we determine the moment matrix

$$(2.16) \quad M_j^\nu := \left[ \int_{\Gamma} (x - x_0)^\alpha \Phi_{j+1}^\nu(x) d\Gamma \right]_{|\alpha| < \tilde{d}}$$

of the cluster  $\nu$  from the level  $j$ . Employing the singular value decomposition

$$(2.17) \quad M_j^\nu = U \Sigma V^\top = U [S, 0] [V_{j,0}^\nu, V_{j,1}^\nu]^\top$$

we obtain the coefficient matrices  $V_{j,0}^\nu$  and  $V_{j,1}^\nu$ , cf. [17].

In the next theorem we prove the approximation property with respect to spaces  $V_j$ . To that end, we have to assume the boundary  $\Gamma$  to be simply connected.

**Theorem 2.1** (Approximation property). *Let the boundary  $\Gamma$  be simply connected. Then, the spaces  $V_j$  defined via (2.14), (2.15), and (2.17) satisfy the approximation property*

$$\inf_{v_j \in V_j} \|v - v_j\|_s \lesssim 2^{j(s-t)} \|v\|_t$$

for all  $s \leq t \leq 1$  uniformly in  $j$ .

*Proof.* On each cluster  $\nu_j$  we can represent the projections of the traces of all polynomials up to the degree  $\tilde{d} \geq 1$  onto the piecewise constant functions with respect to the finest grid, in particular the constant function, which gives us the characteristic function  $\chi_{\nu_j}$ . Employing local Lipschitz continuous coordinates and observing that constant functions are preserved under bi-Lipschitz continuous coordinate transforms, by Bramble-Hilbert theory (see e.g. [4]) we conclude the well known approximation property

$$\inf_{v_j \in V_j} \|v - v_j\|_0 \lesssim 2^{-j} \|v\|_1.$$

By standard arguments we obtain the general result.  $\square$

Next, to proof the Bernstein inequality we make use of local Lipschitz continuous coordinates. For sake of simplicity, we assume that each cluster  $\nu$  has a regular parametric representation, i.e., there exists a domain  $U_\nu \subset \mathbb{R}^n$  and a Lipschitz continuous diffeomorphism such that  $\kappa_\nu(U_\nu) = V_\nu \subset \Gamma$ , where  $V_\nu$  denotes a sufficiently large neighbourhood of the cluster  $\nu$ . The preimage of the cluster itself is indicated by  $\Omega_\nu$ , that is  $\Omega_\nu := \kappa_\nu^{-1}(\nu)$ . Without loss of generality we assume  $\kappa_\nu(x) \sim 1$  for all  $x \in U_\nu$  which can be realized by rescaling. In particular, this condition implies  $\text{diam } \Omega_\nu \sim \text{diam } \nu$ . At least from a certain level, the aforementioned assumptions are valid.

With these preparations at hand we can compute the first order  $L^2$ -modulus of smoothness defined by

$$\omega_1(\phi_i^\nu, t)_2 := \sup_{\|h\| \leq t} \sqrt{\int_{U_\nu} |(\phi_i^\nu \circ \kappa_\nu)(x) - (\phi_i^\nu \circ \kappa_\nu)(x - h)|^2 dx}$$

of the scaling functions for  $t \lesssim \text{diam } U_\nu$ . For  $t \gtrsim \text{diam } U_\nu$  we simply set  $\omega_1(\phi_i^\nu, t)_2 \sim 1$ .

**Lemma 2.2** (Bernstein inequality). *The first order  $L^2$ -modulus of smoothness with respect to the scaling functions satisfies*

$$\omega_1(\phi_i^\nu, t)_2 \lesssim \min \{1, \sqrt{t / \text{diam } \nu}\}.$$

*Proof.* If  $t \geq \text{diam } \Omega_\nu$ , then the supports of  $\phi_i^\nu \circ \kappa_\nu$  and  $(\phi_i^\nu \circ \kappa_\nu)(\cdot - h)$  are disjoint which leads to

$$(2.18) \quad \omega_1(\phi_i^\nu, t)_2 \leq 2 \|\phi_i^\nu\|_{L^2(\Gamma)} = 2.$$

Next, we assume  $t \leq \text{diam } \Omega_\nu$ . Abbreviating

$$\Omega_\nu^h := \text{supp} \left( (\phi_i^\nu \circ \kappa_\nu)(\cdot - h) \right),$$

we find the identity

$$\begin{aligned} \omega_1(\phi_i^\nu, t)_2^2 = \sup_{\|h\| \leq t} & \left\{ \int_{\Omega_\nu \setminus \Omega_\nu^h} |(\phi_i^\nu \circ \kappa_\nu)(x)|^2 dx + \int_{\Omega_\nu^h \setminus \Omega_\nu} |(\phi_i^\nu \circ \kappa_\nu)(x - h)|^2 dx \right. \\ & \left. + \int_{\Omega_\nu^h \cap \Omega_\nu} |(\phi_i^\nu \circ \kappa_\nu)(x) - (\phi_i^\nu \circ \kappa_\nu)(x - h)|^2 dx \right\}. \end{aligned}$$

First, we estimate

$$|\Omega_\nu \setminus \Omega_\nu^h| \lesssim \|h\| (\text{diam } \Omega_\nu)^{n-1} \leq t (\text{diam } \Omega_\nu)^{n-1},$$

which gives

$$\begin{aligned} \int_{\Omega_\nu \setminus \Omega_\nu^h} |(\phi_i^\nu \circ \kappa_\nu)(x)|^2 dx & \lesssim t (\text{diam } \Omega_\nu)^{n-1} \|\phi_i^\nu \circ \kappa_\nu\|_{L^\infty(U_\nu)}^2 \\ (2.19) \qquad \qquad \qquad & = t (\text{diam } \Omega_\nu)^{n-1} \|\phi_i^\nu\|_{L^\infty(\Gamma)}^2. \end{aligned}$$

Likewise, we obtain

$$\begin{aligned} \int_{\Omega_\nu^h \setminus \Omega_\nu} |(\phi_i^\nu \circ \kappa_\nu)(x - h)|^2 dx & \lesssim t (\text{diam } \Omega_\nu^h)^{n-1} \|(\phi_i^\nu \circ \kappa_\nu)(\cdot - h)\|_{L^\infty(U_\nu)}^2 \\ (2.20) \qquad \qquad \qquad & \lesssim t (\text{diam } \Omega_\nu)^{n-1} \|\phi_i^\nu\|_{L^\infty(\Gamma)}^2 \end{aligned}$$

since  $|\Omega_\nu^h| = |\Omega_\nu|$  and  $\|\kappa_\nu\|_{L^\infty(U_\nu)} \lesssim 1$ .

The restrictions  $(x - x_0)^\alpha|_\Gamma$ ,  $\alpha < \tilde{d}$ , are Lipschitz continuous on  $V_\nu$ . The projections of these traces onto the piecewise constant functions with respect to the finest grid define a  $\tilde{d}$ -dimensional vector space. Since  $\phi_i^\nu \circ \kappa_\nu$  is contained in this space we obtain the following estimate

$$(2.21) \quad \int_{\Omega_\nu^h \cap \Omega_\nu} |(\phi_i^\nu \circ \kappa_\nu)(x) - (\phi_i^\nu \circ \kappa_\nu)(x - h)|^2 dx \lesssim t^2 (\text{diam } \Omega_\nu)^n \|\phi_i^\nu\|_{L^\infty(\Gamma)}^2,$$

analogously to the approximation of Lipschitz functions by piecewise constant functions. Notice that we have also used

$$|\Omega_\nu^h \cap \Omega_\nu| \lesssim (\text{diam } \Omega_\nu)^n.$$

Combining (2.19)–(2.21), and observing  $t \leq \text{diam } \Omega_\nu \lesssim 2^{-j}$ , we arrive at

$$\omega_1(\phi_i^\nu, t)_2^2 \lesssim t (\text{diam } \Omega_\nu)^{n-1} (2 + t \text{diam } \Omega_\nu) \|\phi_i^\nu\|_{L^\infty(\Gamma)}^2 \lesssim t (\text{diam } \Omega_\nu)^{n-1} \|\phi_i^\nu\|_{L^\infty(\Gamma)}^2.$$

Finally, we employ that a cluster  $\nu$  on the level  $j$  has been supposed to consist of  $2^{(J-j)n}$  panels (cf. Subsection 2.1) which implies that  $|\Omega_\nu| \sim 2^{(J-j)n}$ . Consequently, we deduce  $\|\phi_i^\nu\|_{L^\infty(\Gamma)} \lesssim 2^{jn/2} \sim (\text{diam } \Omega_\nu)^{-n/2}$  and hence

$$\omega_1(\phi_i^\nu, t)_2^2 \lesssim \frac{t}{\text{diam } \Omega_\nu},$$

which is together with (2.18) the assertion since  $\text{diam } \Omega_\nu \sim \text{diam } \nu$ .  $\square$

Using the equivalence of Sobolev and Besov norms for  $0 < s < 1/2$ , the Bernstein inequality implies the inverse estimate, cf. [3] for example.

**Corollary 2.3** (Inverse estimate). *The spaces  $V_j$  defined via (2.14), (2.15), and (2.17) satisfy the inverse estimate*

$$\|v_j\|_t \lesssim 2^{j(s-t)} \|v_j\|_s, \quad v_j \in V_j,$$

for all  $-1/2 < s \leq t < 1/2$ .

The present algorithm computes recursively defined wavelet functions. In addition to the wavelets we have to add the scaling functions of the coarsest cluster to get a complete basis. Hence, the wavelet basis is defined by

$$\Psi_N := \Phi_0^\Gamma \cup \{\Psi_j^\nu : \nu \in T\}.$$

The next theorem specifies the important properties of our wavelet basis.

**Theorem 2.4.** *The wavelets  $\{\Psi_N\}$  define an orthonormal basis with respect to the inner product (1.2). The amount of wavelets on the level  $j$  is approximately  $2^{jn}$  while the diameter of their support scales like  $2^{-j}$ . The wavelets provide vanishing moments in terms of (2.13) of order  $\tilde{d}$ .*

*Proof.* The orthogonality is an immediate consequence of the construction, see also [17]. Further, in each cluster  $\nu$  of the level  $j$ , we obtain  $\mathcal{O}(1)$  wavelets  $\{\psi_{j,k}^\nu\}$  independently from  $N$  and the level  $j$ , which are supported in the cluster  $\nu$ . Since we have  $\sim 2^{jn}$  clusters with diameter  $\sim 2^{-j}$  on each level  $j$  we have proven the second assertion.

Because  $V$  is orthogonal, (2.17) is equivalent to

$$U[S, 0] = M_j^\nu [V_{j,0}^\nu, V_{j,1}^\nu].$$

Inserting the definition (2.16) we find

$$\begin{aligned} [US, 0] &= \left[ \int_\Gamma (x - x_0)^\alpha \Phi_{j+1}^\nu(x) d\Gamma \right]_{|\alpha| < \tilde{d}} [V_{j,0}^\nu, V_{j,1}^\nu] \\ &= \left[ \left[ \int_\Gamma (x - x_0)^\alpha \Phi_{j+1}^\nu(x) d\Gamma \right]_{|\alpha| < \tilde{d}} V_{j,0}^\nu, \left[ \int_\Gamma (x - x_0)^\alpha \Phi_{j+1}^\nu(x) d\Gamma \right]_{|\alpha| < \tilde{d}} V_{j,1}^\nu \right] \\ &= \left[ \left[ \int_\Gamma (x - x_0)^\alpha \Phi_j^\nu(x) V_{j,0}^\nu d\Gamma \right]_{|\alpha| < \tilde{d}}, \left[ \int_\Gamma (x - x_0)^\alpha \Phi_j^\nu(x) V_{j,0}^\nu d\Gamma \right]_{|\alpha| < \tilde{d}} \right]. \end{aligned}$$

Using the refinement relation (2.14) we arrive at

$$(2.22) \quad \begin{aligned} \left[ \int_\Gamma (x - x_0)^\alpha \Phi_j^\nu(x) d\Gamma \right]_{|\alpha| < \tilde{d}} &= US, \\ \left[ \int_\Gamma (x - x_0)^\alpha \Psi_j^\nu(x) d\Gamma \right]_{|\alpha| < \tilde{d}} &= 0, \end{aligned}$$



that is the proof of (2.13). □

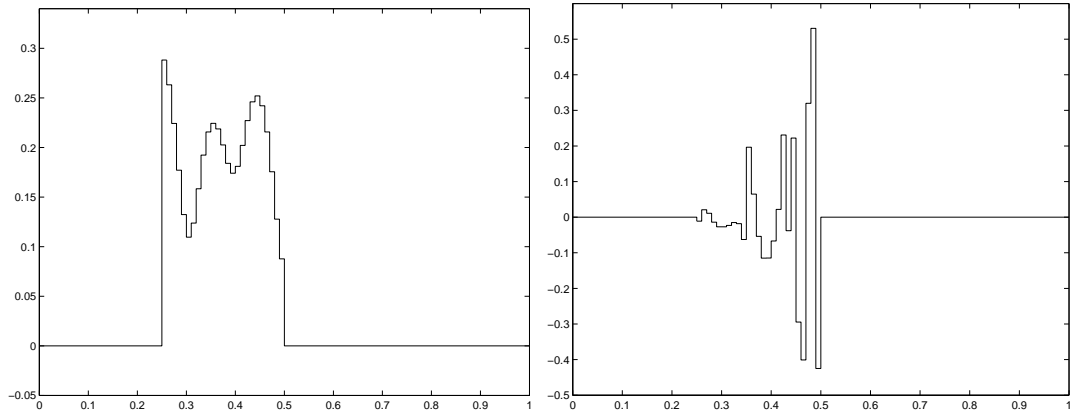


FIGURE 2.2. A scaling function (left) and a wavelet with three vanishing moments (right).

The construction of wavelets starts on the finest level where we can determine all moment matrices directly within  $\mathcal{O}(N)$  operations. In every cluster we have to compute the singular value decomposition of the moment matrix to get the coefficients of the wavelets and the coarse grid scaling functions as well as their moments, cf. (2.22). These moments can be reused for the further computations after transferring them to the center of the father cluster. Because of our assumptions on the cluster tree we have  $\mathcal{O}(N)$  clusters in all and consequently an over-all complexity for the construction of the wavelet basis of  $\mathcal{O}(N)$ . A wavelet with three vanishing moments and a corresponding scaling function can be found in Figure 2.2.

In the sequel we will make use of the following renumbering. All scaling functions and wavelets on the level  $j$  will be called  $\phi_{j,k}$  and  $\psi_{j,k}$ , respectively, where  $k$  is from a suitable index set of cardinality  $\sim 2^{jn}$ . Remember that the scaling functions and wavelets on the level  $j$  are always supported in a single cluster from the same level.

Following [5, 8], the approximation property (Theorem 2.1) together with the Bernstein inequality (Lemma 2.2) prove the norm equivalence in the range  $|s| < 1/2$ .

**Corollary 2.5** (Norm equivalence). *Let the boundary  $\Gamma$  be simply connected. Then, for  $|s| < 1/2$  and  $v \in H^{\max\{s,0\}}(\Gamma)$  there holds the norm equivalence*

$$\|v\|_{H^s(\Omega)}^2 \sim \sum_{j,k} 2^{js} |\langle v, \psi_{j,k} \rangle|^2.$$

According to [13], as a consequence of this norm equivalence, we obtain the following result.

**Proposition 2.6.** *Let  $\mathbf{A}_N^\psi = [\langle A\psi_{j',k'}, \psi_{j,k} \rangle]_{(j,k),(j',k')}$  denote the Galerkin matrix in wavelet coordinates corresponding to the single layer operator. The condition number of the diagonally preconditioned system matrix grows only polylogarithmically*

$$\text{cond} \left( (\text{diag } A_N^\psi)^{-1/2} A_N^\psi (\text{diag } A_N^\psi)^{-1/2} \right) \lesssim \log^2 N.$$

**2.3. Discrete wavelet transform.** In order to solve (1.1) by the wavelet Galerkin scheme it will be necessary to switch between the wavelet and the single-scale representations

$$f_j = \sum_{j,k} \langle f, \psi_{j,k} \rangle \psi_{j,k} = \sum_i \langle f, \phi_i \rangle \phi_i.$$

Likewise to the wavelet construction, we can determine the coefficients recursively via the fast wavelet transform

$$[\langle f, \Phi_j^\nu \rangle, \langle f, \Psi_j^\nu \rangle] = \langle f, \Phi_{j+1}^\nu \rangle [V_{j,0}^\nu, V_{j,1}^\nu], \quad j = J, J-1, \dots, 0,$$

which scales linearly. Due to the orthogonality of  $[V_{j,0}^\nu, V_{j,1}^\nu]$  we can pass backwards through this algorithm to gain the inverse wavelet transform. For further details we refer to [14, 17].

### 3. THE WAVELET GALERKIN SCHEME

**3.1. Wavelet matrix compression.** The idea of the wavelet Galerkin scheme is just to use the wavelet basis  $\Psi_J$  for the discretization of (1.9). Making the ansatz  $u_N = \sum_{j,k} u_{j,k} \psi_{j,k}$  and defining  $\mathbf{A}_N^\psi = [\langle A\psi_{j',k'}, \psi_{j,k} \rangle]_{(j,k),(j',k')}$ ,  $\mathbf{u}_N^\psi = [u_{j,k}]_{(j,k)}$ , and  $\mathbf{f}_N^\psi = [\langle f, \psi_{j,k} \rangle]_{(j,k)}$ , we arrive at the linear system of equations

$$(3.23) \quad \mathbf{A}_N^\psi \mathbf{u}_N^\psi = \mathbf{f}_N^\psi.$$

We denote the convex hull to the support of the wavelet  $\psi_{j,k}$  by  $\Theta_{j,k}$ . Note that, in general,  $\Theta_{j,k}$  is just the convex hull of the associated cluster since the support of the wavelet is identical to this cluster. Employing the Taylor expansion of the kernel

(1.6), (1.7) we can estimate the size of a single matrix coefficient

$$\begin{aligned}
|\langle A\psi_{j',k'}, \psi_{j,k} \rangle| &\lesssim \left| \sum_{\min\{|\alpha|, |\beta|\} < \tilde{d}} \frac{\partial_x^\alpha \partial_y^\beta k(x_0, y_0)}{\alpha! \beta!} \right. \\
&\quad \cdot \underbrace{\int_{\Gamma} (x - x_0)^\alpha \psi_{j,k}(x) d\Gamma}_{=0} \underbrace{\int_{\Gamma} (y - y_0)^\beta \psi_{j',k'}(y) d\Gamma}_{=0} \left. \right| \\
&+ \left| \frac{2^{-(j+j')\tilde{d}}}{[s \operatorname{dist}(\Theta_{j,k}, \Theta_{j',k'})]^{n+2q+2\tilde{d}}} \int_{\Gamma} |\psi_{j,k}(x)| d\Gamma \int_{\Gamma} |\psi_{j',k'}(y)| d\Gamma \right| \\
&\lesssim \frac{2^{-(j+j')(\tilde{d}+n/2)}}{\operatorname{dist}(\Theta_{j,k}, \Theta_{j',k'})^{n+2q+2\tilde{d}}}
\end{aligned}$$

provided that  $\operatorname{dist}(\Theta_{j,k}, \Theta_{j',k'}) > 0$ . That is, the system matrix  $\mathbf{A}_N^\psi$  is now quasi-sparse. Employing wavelets with enough vanishing moments most of the matrix coefficients can be discarded without compromising the stability and accuracy of the underlying Galerkin scheme. Setting all matrix coefficients to zero for which the distance of the support of the corresponding ansatz and test functions is bigger than a level dependent cut-off parameter  $\mathcal{B}_{j,j'}$  is called wavelet compression. For given parameters

$$(3.24) \quad a > 1, \quad d < d' < \tilde{d} + 2q,$$

we define the cut-off parameter  $\mathcal{B}_{j,j'}$  as

$$(3.25) \quad \mathcal{B}_{j,j'} := a \max \left\{ 2^{-\min\{j,j'\}}, 2^{\frac{2J(d'-q)-(j+j')(d'+\tilde{d})}{2(\tilde{d}+q)}} \right\}.$$

**Theorem 3.1.** *The system matrix  $\mathbf{A}_N^\psi$  can be compressed in accordance with*

$$(3.26) \quad \left[ \mathbf{A}_N^\psi \right]_{(j,k),(j',k')} := \begin{cases} 0, & \text{if } \operatorname{dist}(\Theta_{j,k}, \Theta_{j',k'}) > \mathcal{B}_{j,j'}, \\ \langle A\psi_{j',k'}, \psi_{j,k} \rangle & \text{otherwise,} \end{cases}$$

to only  $\mathcal{O}(N \log N)$  nonzero matrix coefficients without compromising the stability and accuracy of the underlying Galerkin scheme.

*Proof.* The stability and accuracy of the wavelet Galerkin scheme is an immediate consequence of the analysis presented in [7, 15].

Next, we estimate the number of nonzero coefficients in the compressed system matrix. For fixed levels  $j$  and  $j'$  we find only  $2^{(j+j')n} \mathcal{B}_{j,j'}^n$  nonzero matrix coefficients. Setting  $M := \frac{d'+\tilde{d}}{2(\tilde{d}+q)}$  and observing

$$2^{-J} 2^{(J-j)M} 2^{(J-j')M} = 2^{\frac{2J(d'-q)-(j+j')(d'+\tilde{d})}{2(\tilde{d}+q)}},$$

we can rewrite the cut-off parameter

$$\mathcal{B}_{j,j'} \sim \max \left\{ 2^{-\min\{j,j'\}}, 2^{-J} 2^{(J-j)M} 2^{(J-j')M} \right\}.$$

We count first all coefficients  $\langle A\psi_{j',k'}, \psi_{j,k} \rangle$  for which

$$\text{dist}(\Theta_{j,k}, \Theta_{j',k'}) \lesssim 2^{-J} 2^{(J-j)M} 2^{(J-j')M}.$$

This number is bounded by

$$\sum_{j,j'=0}^J 2^{(j+j')n} 2^{-Jn} 2^{(J-j)Mn} 2^{(J-j')Mn} = 2^{Jn} \sum_{j,j'=0}^J 2^{(J-j)(M-1)n} 2^{(J-j')(M-1)n} \lesssim 2^{Jn},$$

since  $M < 1$  due to (3.24). It remains to count the number of coefficients for which

$$\text{dist}(\Theta_{j,k}, \Theta_{j',k'}) \lesssim 2^{-\min\{j,j'\}}.$$

In the case  $j \geq j'$  this number is bounded by

$$\sum_{j=0}^J \sum_{j'=0}^j 2^{(j+j')n} 2^{-j'n} = \sum_{j=0}^J 2^{jn} (j+1) \lesssim 2^{Jn} J,$$

and likewise for  $j \leq j'$ . Due to  $N \sim 2^{Jn}$  and  $\log N \sim J$  this finishes the proof.  $\square$

The compression pattern generated by the wavelet matrix compression in case of the single layer operator and  $n = 1$  are plotted in Figure 3.3. Notice that the very unusual structure issues from the recursive numbering of the wavelets. A reordering will lead to the well known finger structure.

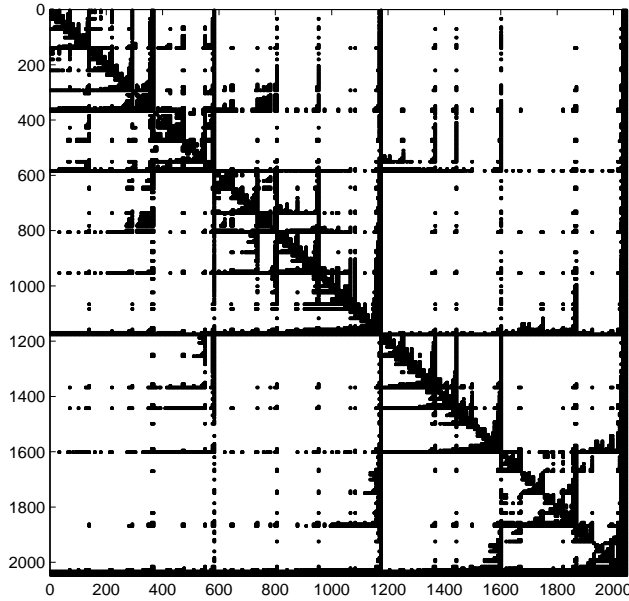


FIGURE 3.3. Compression pattern of the system matrix ( $N = 2048$ ).

**3.2. Setting up the matrix pattern.** A naive check of the distance criterion (3.26) for each matrix coefficient results in a  $\mathcal{O}(N^2)$ -procedure. To realize sub-linear complexity, we exploit the underlying tree structure with respect to the supports of the wavelets, to predict negligible matrix coefficients. We will call a wavelet  $\psi_{j+1,\text{son}}$  a son of  $\psi_{j,\text{father}}$  if  $\Theta_{j+1,\text{son}} \subseteq \Theta_{j,\text{father}}$ . This father-son relation corresponds to the father-son relation of the associated clusters.

**Lemma 3.2.** *For  $\Theta_{j+1,\text{son}} \subseteq \Theta_{j,\text{father}}$  and  $\Theta_{j'+1,\text{son}} \subseteq \Theta_{j',\text{father}}$  the relation*

$$\text{dist}(\Theta_{j,\text{father}}, \Theta_{j',\text{father}}) > \mathcal{B}_{j,j'}$$

*implies*

$$\text{dist}(\Theta_{j+1,\text{son}}, \Theta_{j',\text{father}}) > \mathcal{B}_{j+1,j'}, \quad \text{dist}(\Theta_{j+1,\text{son}}, \Theta_{j'+1,\text{son}}) > \mathcal{B}_{j+1,j'+1}.$$

*Proof.* The assertion is an immediate consequence of the relation  $\mathcal{B}_{j,j'} \geq \mathcal{B}_{j+1,j'} \geq \mathcal{B}_{j+1,j'+1}$ .  $\square$

With the aid of this lemma we have to check the distance criteria only for coefficients which stem from subdivisions of calculated coefficients on a coarser level. Therefore, the resulting procedure of checking the distance criteria is still of complexity  $\mathcal{O}(N \log N)$ .

**3.3. Computing the compressed system matrix.** Since the boundary representation is not smooth, we cannot exploit an exponentially convergent  $hp$ -quadrature formula like in [7, 15, 16] to compute the relevant matrix coefficients  $\langle A\psi_{j,k}, \psi_{j',k'} \rangle$ . We propose to employ instead a fast multipole or panel clustering scheme based on the Taylor expansion (1.4) to compute relevant coefficients efficiently.

Since a wavelet  $\psi_{j,k}$  is a finite linear combination of scaling functions from the finer grid (cf. (2.14)), i.e.

$$\psi_{j,k} = \sum_{k'} v_{k'} \phi_{j+1,k'},$$

it suffices to provide a method to compute the interactions of scaling functions  $\langle A\phi_{j',k'}, \phi_{j,k} \rangle$ .

If the relative distance of the associated clusters  $\nu_j$  and  $\nu_{j'}$  is large enough

$$(3.27) \quad \text{dist}(\nu_j, \nu_{j'}) > \eta \max\{\text{diam } \nu_j, \text{diam } \nu_{j'}\} \sim 2^{-\min\{j,j'\}} \eta, \quad \eta > \frac{1}{s},$$

then we can exploit the Taylor expansion (1.4) in the centroids  $x_0 \in \nu_j$  and  $y_0 \in \nu_{j'}$

$$(3.28) \quad \langle A\phi_{j',k'}, \phi_{j,k} \rangle \approx \sum_{|\alpha|, |\beta| < p} \frac{\partial_x^\alpha \partial_y^\beta k(x_0, y_0)}{\alpha! \beta!} \cdot \int_{\Gamma} (x - x_0)^\alpha \phi_{j,k}(x) d\Gamma \int_{\Gamma} (y - y_0)^\beta \phi_{j',k'}(y) d\Gamma,$$

where the error  $\varepsilon$  is bounded by (cf. (1.5))

$$|\varepsilon| \lesssim \frac{\max\{\text{diam } \nu_j, \text{diam } \nu_{j'}\}^p (\text{diam } \nu_j)^{n/2} (\text{diam } \nu_{j'})^{n/2}}{[s \text{ dist}(\nu_j, \nu_{j'})]^{n+2q+p}} \lesssim \frac{2^{-(j+j')n/2}}{(s\eta)^{n+2q+p}}.$$

Providing precomputed moments

$$M_{j,k} := \left[ \int_{\Gamma} (x - x_0)^\alpha \phi_{j,k}(x) d\Gamma \right]_{|\alpha| < p},$$

the evaluation of (3.28) requires  $p^{2(n+1)}$  operations.

If (3.27) is violated then we have to subdivide the larger cluster into its son cluster if  $j \neq j'$  or divide both if  $j = j'$ . This can be performed by inserting the refinement relation (2.14) for the scaling functions. Then, one has to check again the admissibility condition (3.27) for all appearing integrals to make a decision which values can be computed directly by (3.28) and which one have again to be subdivided. Of course, the depth of subdivision is bounded by  $\max\{J - j, J - j'\}$  since on the finest level  $J$  one computes the near field directly by numerical quadrature. Since on each stage at most  $\mathcal{O}(1)$  interactions violate the admissibility condition (3.27) the number of computed coefficients is bounded by  $\mathcal{O}(J)$ . It is well known that the degree  $p$  has to be chosen  $\sim \log N \sim J$  to achieve a certain accuracy  $N^{-\alpha}$ ,  $\alpha > 0$ . Hence, the computation of a single matrix coefficient requires at most  $\mathcal{O}(\log^{2(n+1)+1} N)$  operations. Consequently, the computation of the compressed system matrix requires at most  $\mathcal{O}(N \log^{2(n+2)} N)$  operations.

**Remark 3.3.** *This complexity estimate is rather crude. For example, in three dimensions, using a Taylor expansion of the kernel based on spherical harmonics, we can reduce the complexity per coefficient to  $\mathcal{O}(N \log^{2n+1} N)$ .*

*Next, we emphasize that the full accuracy is required only for the interactions on the coarsest grid. As shown in [7] it suffices to compute a single interaction  $\langle A\phi_{j',k'}, \phi_{j,k} \rangle$  with a level dependent accuracy*

$$(3.29) \quad \varepsilon_{j,j'} \sim \min \left\{ 2^{-\frac{|j-j'|n}{2}}, 2^{-n(J - \frac{j+j'}{2}) \frac{d'-q}{d+q}} \right\} 2^{2Jq} 2^{-2d'(J - \frac{j+j'}{2})}$$

*with  $d' \in (1, \tilde{d} + 2q)$  from (3.24). Further, we can exploit different expansion degrees in the variables if associated clusters belong to different levels. We are convinced that incorporating these items we can reduce again the polylogarithmical term. Also*

more recent fast multipole versions can be applied for a further reduction. Of course, since we use the fast multipole method or a similar method for the computation of the compressed system matrix, the complexity of these methods is inherent in the precomputational step of matrix generation.

#### 4. NUMERICAL RESULTS

This last section is dedicated to a numerical example for the case of two space dimensions ( $n = 1$ ). Let  $\Gamma$  be defined as the equidistant piecewise linear and continuous approximation of the following boundary curve

$$\gamma : [0, 1] \rightarrow \Gamma, \quad \gamma(t) = \frac{1}{20}(4 + \cos(10\pi t) + \cos(2\pi t)) \begin{bmatrix} \cos(2\pi t) \\ \sin(2\pi t) \end{bmatrix}.$$

Note that this curve underlies the clustering in Figure 2.1. On the domain  $\Omega$  which is bounded by  $\Gamma$  we want to solve an interior Dirichlet problem for the Laplacian. For a given function  $f \in H^{-1/2}(\Gamma)$  we seek  $u \in H^1(\Omega)$  such that

$$(4.30) \quad \begin{aligned} \Delta u &= 0 && \text{in } \Omega, \\ u &= f && \text{on } \Gamma. \end{aligned}$$

Choosing the harmonical function

$$U(x) = e^{x_1} \cos(x_2)$$

and setting  $f := U|_{\Gamma}$ , the function  $U$  is the unique solution of (4.30).

We consider the indirect formulation for the single respective double layer operator. Firstly, employing the single layer operator

$$(V\rho)(x) := -\frac{1}{2\pi} \int_{\Gamma} \log \|x - y\| \rho(y) d\Gamma(y), \quad x \in \Gamma,$$

we arrive at a Fredholm integral equation of the first kind for an unknown density  $\rho \in H^{-1/2}(\Gamma)$

$$(4.31) \quad V\rho = f \quad \text{on } \Gamma.$$

With this density at hand the solution  $u \in \Omega$  is given by the potential evaluation

$$u(x) = (V\rho)(x), \quad x \in \Omega.$$

Secondly, the double layer operator

$$(K\rho)(x) := \frac{1}{2\pi} \int_{\Gamma} \frac{\langle n(y), y - x \rangle}{\|y - x\|^2} \rho(y) d\Gamma(y), \quad x \in \Gamma,$$

yields a Fredholm integral equation of the second kind

$$(4.32) \quad (K - \frac{1}{2}I)\rho = f \quad \text{on } \Gamma$$

for the unknown density  $\rho$ . Therewith, the solution of (4.30) can be represented by the potential evaluation

$$u(x) = (K\rho)(x), \quad x \in \Omega.$$

Note that the operators appearing on the left hand side of (4.31) and (4.32) denote operators of the order  $-1$  and  $0$ , respectively.

We discretize the integral equations (4.31) and (4.32) by the traditional single-scale basis and the constructed wavelet basis. The resulting systems are solved iteratively by CG or GMRES. We compute the approximate solutions to  $\rho$  by the traditional single-scale Galerkin scheme, a multipole scheme which just replaces the matrix-vector multiplication by a fast approximation, and the compressed wavelet Galerkin scheme. The wavelets have to provide  $\tilde{d} = 3$  and  $\tilde{d} = 2$  vanishing moments in case of the single and double layer operator, respectively.

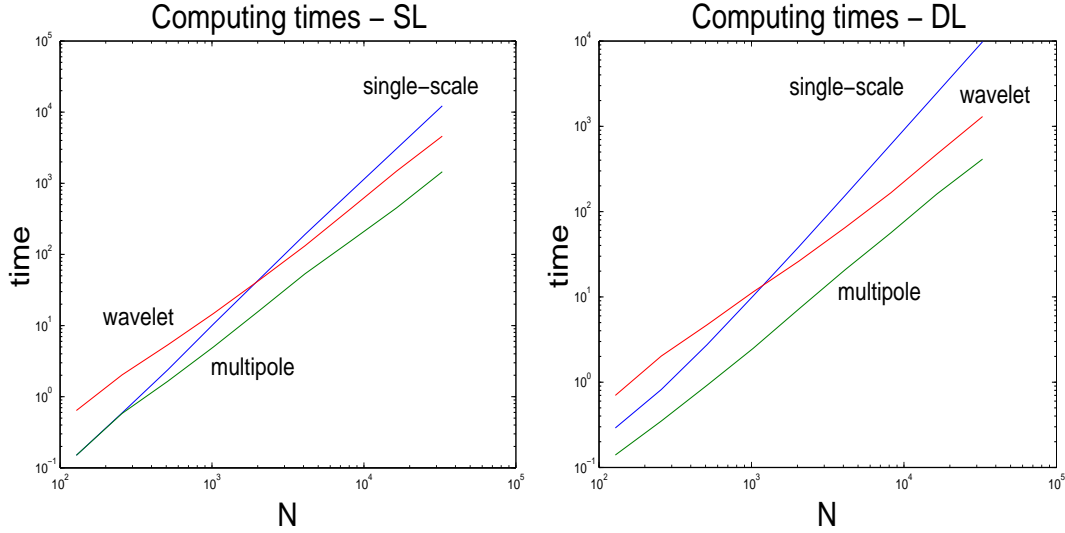


FIGURE 4.4. Computing times with respect to the single layer operator (left) and the double layer operator (right).

First, we compare the over-all computing time of the three methods for achieving the solution  $u_N$  within discretization error

$$\epsilon_N = \max_i |u(\xi_i) - u_N(\xi_i)|$$

for a set  $\{\xi_i\}$  of fixed points distributed in the domain  $\Omega$ . Note that  $\epsilon_N \lesssim N^{-3}$  and  $\epsilon_N \lesssim N^{-2}$  for the single and double layer operator, respectively, provided that  $\rho$  is smooth enough, cf. [18].

Figure 4.4 is concerned with the over-all computing times. We can see the asymptotical inferiority of the single-scale method compared to the other two methods. Admittedly, Figure 4.4 shows that the present wavelet Galerkin method is about a



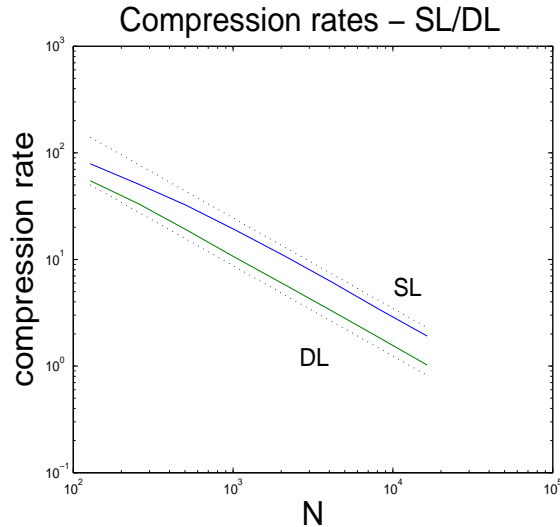


FIGURE 4.5. Percentage of relevant coefficients in the compressed system matrix.

factor three slower than the multipole method. This effect issues from the fact that we apply the fast multipole method for matrix generation. However, the wavelet compression yields a significant sparsification of the system matrix. In Figure 4.5 the straight lines indicate the ratio of the number of relevant coefficients and the dense matrix, that is  $N^2$ . The dotted lines correspond to a linear behaviour.

We shall next compare the setup time versus the solving time in the case of the double layer operator. In case of the wavelet Galerkin method the computation of the system matrix has to be performed only once which requires the major part of the computing time (left plot of Figure 4.6). Nevertheless, the time for solving the quite sparse system iteratively is nearly negligible since it just requires usual matrix-vector multiplications. The behaviour of the multipole method is opposite: preparation and iterative solution are balanced (right plot of Figure 4.6). However, the cpu-time time of the multipole method heavily depends on the number of iterations which is governed by the condition number of the arising system matrix. This means that, particularly for operators of nonzero order in case of  $n = 2$ , the solving time can increase dramatically. Whereas, the time spent on the iterative solution of the compressed wavelet Galerkin system, even without wavelet preconditioning, will be only a minor part of the over-all computing time.

These properties demonstrate an advantage of the wavelet Galerkin method, namely the fast solution of the associated linear system of equations for multiple right hand sides. In particular, we may conclude that from a certain amount (about five in the present example) of right hand sides the present wavelet Galerkin method becomes faster than the multipole method.

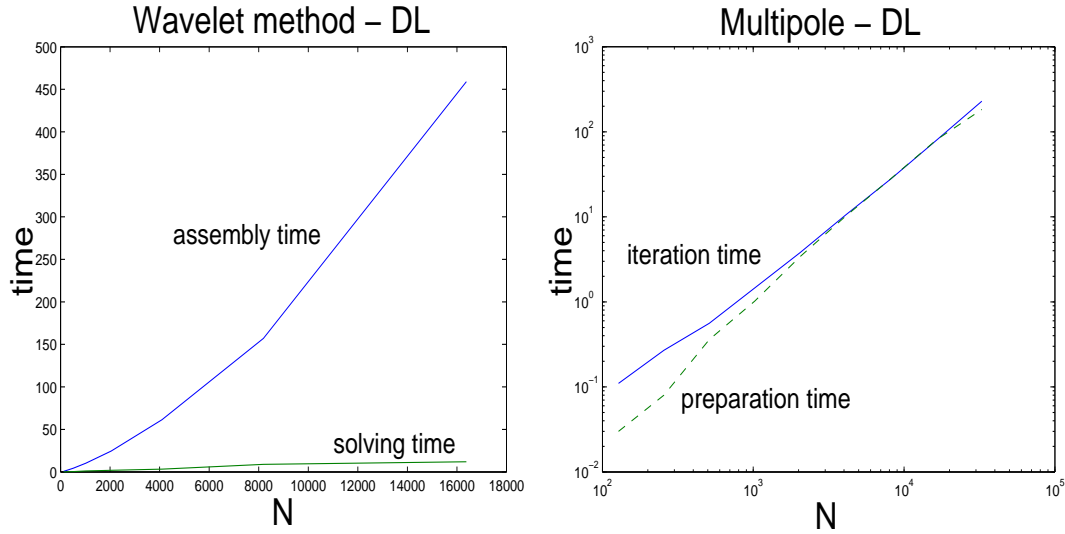


FIGURE 4.6. Times for the setup versus the solving in case of the wavelet Galerkin scheme (left) and the fast multipole method (right).

#### REFERENCES

- [1] M. Bebendorf and S. Rjasanow. Adaptive low-rank approximation of collocation matrices. *Computing*, 70, No.1, 1–24, 2003.
- [2] G. Beylkin, R. Coifman, and V. Rokhlin. The fast wavelet transform and numerical algorithms. *Comm. Pure and Appl. Math.*, 44:141–183, 1991.
- [3] A. Cohen. *Numerical analysis of wavelet methods*. Studies in Mathematics and its Applications, 32. North-Holland, Amsterdam, 2003.
- [4] P.G. Ciarlet. *The Finite Element Method for Elliptic Problems*. North Holland, Amsterdam, 1978.
- [5] W. Dahmen. Stability of multiscale transformations. *Journal of Fourier Analysis and Applications*, 2:341–361, 1996.
- [6] W. Dahmen. Wavelet and multiscale methods for operator equations. *Acta Numerica*, 6:55–228, 1997.
- [7] W. Dahmen, H. Harbrecht and R. Schneider. Compression techniques for boundary integral equations – optimal complexity estimates. *Preprint SFB 393/02-06, TU Chemnitz*, 2002. submitted to SIAM J. Numer. Anal.
- [8] W. Dahmen and A. Kunoth. Multilevel preconditioning. *Numer. Math.*, 63:315–344, 1992.
- [9] W. Dahmen, A. Kunoth, and K. Urban. Biorthogonal spline-wavelets on the interval – stability and moment conditions. *Appl. Comp. Harm. Anal.*, 6:259–302, 1999.
- [10] L. Greengard and V. Rokhlin. A fast algorithm for particle simulation. *J. Comput. Phys.*, 73:325–348, 1987.
- [11] W. Hackbusch and B.N. Khoromskij. A sparse  $\mathcal{H}$ -matrix arithmetic. II: Application to multi-dimensional problems. *Computing*, 64:21–47, 2000.

- [12] W. Hackbusch and Z.P. Nowak. On the fast matrix multiplication in the boundary element method by panel clustering. *Numer. Math.*, 54:463–491, 1989.
- [13] P. Oswald. Multilevel norms for  $H^{-1/2}$ . *Computing*, 61:235–255, 1998.
- [14] G. Schmidlin and C. Schwab. Wavelet Galerkin BEM on unstructured meshes by aggregation. *Multiscale and multiresolution methods*, pages 359–378, Lect. Notes Comput. Sci. Eng., 20, Springer, Berlin, 2002.
- [15] R. Schneider. *Multiskalen- und Wavelet-Matrixkompression: Analysisbasierte Methoden zur Lösung großer vollbesetzter Gleichungssysteme*. B.G. Teubner, Stuttgart, 1998.
- [16] C. Schwab. Variable order composite quadrature of singular and nearly singular integrals. *Computing*, 53:173–194, 1994.
- [17] J. Tausch and J. White. Multiscale bases for the sparse representation of boundary integral operators on complex geometries. *SIAM J. Sci. Comput.*, 24:1610–1629, 2003.
- [18] W.L. Wendland, On asymptotic error analysis and underlying mathematical principles for boundary element methods. In C.A. Brebbia, editor, *Boundary Element Techniques in Computer Aided Engineering, NATO ASI Series E - 84*, pages 417–436, Martinus Nijhoff Publ., Dordrecht-Boston-Lancaster, 1984.